MOONQUAKE-TRIGGERED MASS WASTING PROCESSES ON ICY WORLDS. M. M. Mills[1,2], R. T. Pappalardo[2], M. P. Panning[2], E. J. Leonard[2], S. M. Howell[2], [1]Johns Hopkins University, mmills23@jhu.edu, [2]Jet Propulsion Laboratory, California Institute of Technology.

Introduction: Smooth material is prevalent on the surfaces of icy satellites, especially in low topography within ridge and trough terrains, i.e. between subparallel ridge sets. One common origin hypothesis is resurfacing by extrusion and flow of ductile ice [1]. We investigate an alternate hypothesis: creation of smooth material by mass wasting. In this scenario, mass wasted material moves from topographic highs into lows and covers older terrain with smooth material, aided by moonquake-induced seismic shaking as local tectonic ridges are created.

Fault Measurements: To estimate sizes of moonquakes that may have created the observed faults categorize faults, we first employ ArcGIS to create high-resolution geologic maps of each region. On Ganymede, mapping focused on normal faults along the boundaries of Harpagia Sulcus [2]. On Europa, we examine faults within Ino Linea [3]. On Enceladus, we studied inferred normal faults near Harran Sulci [4]. We measure 93 faults on the three bodies: 29 on Ganymede (measured at 16 and 20 m/pixel), 44 on Europa (34 m/pixel), and 14 on Enceladus (85 m/pixel), using Galileo and Cassini images, supplemented by stereo-derived topography [1,4].

We measured two primary dimensions of scarps: length and visible scarp area. Scarps commonly continue into lower resolution context images, so length uncertainties are significant.; thus, measured lengths are minimums and derived quake moments and magnitudes are minimum estimations. From these measured dimensions, we calculated dip-slope length using geometric angle corrections, and we estimated scarp throws using topographic stereo [1,4–6].

Structural Properties: Heave is horizontal displacement along a fault dip-slope, for which we take a cumulative frequency scaling, where (d) is the threshold for all faults with heave less than or equal to a specific value. All three fault populations exhibit approximately linear trends in semi-log space (Fig. 1); thus, all populations are consistent with normal faults extending through their satellite's elastic layer [7].

We also examine displacement-to-length ratios (D/L) of measured scarps, a parameter commonly indicative of brittle material properties and the formational stresses of faults. Because high-resolution data is limited, for the ratio calculations we examined ten faults from each satellite with the entire scarp contained in the images. We find that D/L ratios of Ganymede, Europa, and Enceladus are approximately the same, ranging from 0.01-0.03. They are consistent with ratios measured on mid-ocean spreading centers.

Seismic Calculations: For our calculations, we assumed brittle-ductile transition depths of 2±1 km for all target satellites [4,8,9]. Assuming displacement occurs along the entire scarp, we calculate total scarp area (A) then find seismic moment (M_o) and moment magnitude (M_w) with the following equations:

$$M_o = \mu A s,$$

$$M_w = {}^2/_3 \log(M_o) - 6.06,$$

given a shear modulus (μ = 3.521 GPa [10]) and scarp displacement per event (s). We assume that scarps were built over multiple events [11]; moreover, we assume the s/L ratio is $\approx 5 \times 10^{-4}$ for a single event, and that fault displacement scales linearly with fault length [12–14]. We calculate a seismic moment range of 1.7–6100 x 10^{16} Nm and a moment magnitude range of 4.8–7.1 (Fig. 2). This implies significant available seismic energy during fault formation.

Seismic Models: For seismic modelling, the spectral-element solver AxiSEM was used to read spherical wave-propagation into an azimuthal-directional solution, perpendicular to the receiver plane, which in this case is the icy surface [15–16]. The Python package Instaseis was then used to reconstruct seismograms for arbitrary seismic sources and receivers. We set the sources at approximately 2 km, the adopted brittle-ductile depth. Assuming fault populations penetrate the full elastic zone of each satellite, we can model the quakes originating from this depth. For each satellite, we used a model defined in Green's functions databases for Icy Ocean Worlds [15]. Each model had a hydrated mantle layer at 30 kilometers and an ice shell thickness of 126 km (Ganymede), 20 km (Europa), or 53 km (Enceladus). The degree of seismic shaking is dependent on our estimated seismic moments. Fig. 3 plots modeled vertical acceleration associated with our calculated range of seismic events. Comparing to satellite gravitational accelerations (dashed lines), we see that seismic accelerations can exceed surface gravitational accelerations, especially near quake epicenters. Thus, such seismic events could potentially displace material from topographic highs into topographic lows.

We model potential displaced volumes of our calculated quakes, assuming Earth-based statistics of landslide volume with seismic moment [17]. We estimate mass-wasted volumes, specifically considering the case of 1 Hertz, to be 10^6-10^{10} m^3 for a single

scarp. We propose these volumes of material would have a significant effect on modifying normal-faulted ridge and trough terrains on icy satellites. Given our estimated magnitudes of moonquakes and landslide volumes, we infer that mass wasting is a feasible process for resurfacing surface features on Ganymede, Europa, and Enceladus. The inferred quake strengths can generate seismic accelerations that exceed gravitational acceleration, especially near epicenters.

Acknowledgments: This work was supported by NASA through the Europa Clipper Project.

References: [1] Schenk, P. M. et al., *Nature, 410*, 57–60, 2001. [2] Patel, J. G. et al., *JGR*, *104*, 24057–24074, 1999. [3] Prockter, L. M. et al., *JGR*, *107*, 5028, 10.1029/2000je001458, 2002. [4] Giese, B., et al., *GRL, 35*, 10.1029/2008GL036149, 2008. [5] Bland, M. T. et al., *Icarus, 192*, 92–105, 2017. [6] Nimmo, F., et al., *GRL, 29*, 10.1029/2001GL013976, 2006. [7] Howell, S. M., et al., *G3*, *17*, 2016, 2354–2373. [8] Pappalardo, R. T. et al., *GRL, 25*, 233–236, 1998. [9] Ruiz, J., and Tejero, R., *JGR-Planets*, *105*, 29,283–29,289, 2000. [10] Gammon, P.H. et al., *J. Glaciol., 29*, 433–460, 1983. [11] Nicol, A., et al., *J. Struct. Geol., 27*, 327–342, 2005. [12] Manighetti, I. et al., *JGR, 110*, B05302, 2005. [13] Schultz, R. A., et al., *J. Struct. Geol., 28*, 2182–2193, 2006. [14] Gudmundsson, A., et al., *J. Struct. Geol., 608*, 1298–1309, 2013. [15] Stähler, S. C. et al., *JGR-Planets, 123*, 206–232, 2018. [16] Vance, S. D. et al., *JGR-Planets, 123*, 180–205, 2018. [17] Marc, O., et al., *JGR-Earth*, *121*, 640–663, 2016.

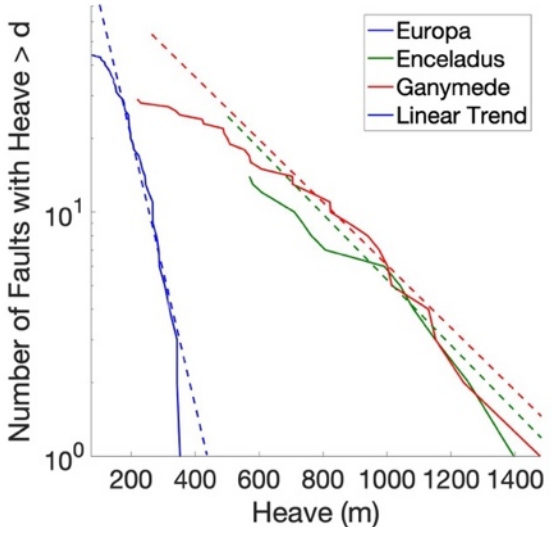

Figure 1: A cumulative scaling of fault heave shows approximately linear trends for all fault populations, indicating normal faults penetrating the elastic layer. Deviations indicate missing faults due to resolution limitations and potential erasure due to mass wasting.

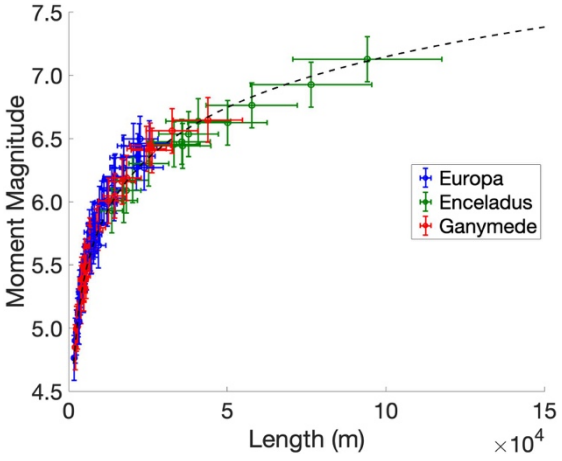

Figure 2. Our distributions of calculated seismic moments and moment magnitudes for each satellite. The logarithmic distribution is because moment magnitude is a logarithmic scaling of seismic moment.

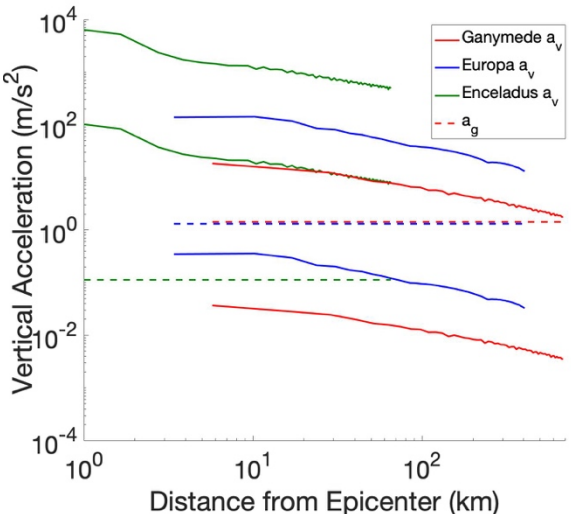

Figure 3: Modeled vertical accelerations resulting from estimated quake sizes. Dashed lines represent surface gravitational acceleration. Solid curves span the range of quake size, the lower curve being the smallest quake we estimated given our measured faults on each satellite, the upper curve being the largest quake we estimated given our measured faults on each satellite. When solid curves exceed the dashed line for each satellite, mass wasting is feasible for moving surface material.